

## Structure-Function Elucidation of a New $\alpha$ -conotoxin, Lo1a, from *Conus longurionis*\*

**Eline K. M. Lebbe<sup>1</sup>; Steve Peigneur<sup>1</sup>; Mohitosh Maiti<sup>2</sup>; Phrabha Devi<sup>3</sup>; S. Ravichandran<sup>4</sup>; Eveline Lescrinier<sup>2</sup>; Etienne Waelkens<sup>5</sup>; Lisette D'Souza<sup>3</sup>; Piet Herdewijn<sup>2</sup>; Jan Tytgat<sup>1</sup>**

<sup>1</sup>Toxicology and Pharmacology, University of Leuven (KU Leuven), Campus Gasthuisberg, O&N2, Herestraat 49, PO Box 922, 3000 Leuven, Belgium

<sup>2</sup>Medicinal Chemistry, University of Leuven (KU Leuven), Rega Institute for Medical Research, Minderbroedersstraat 10, 3000 Leuven, Belgium

<sup>3</sup>CSIR-National Institute of Oceanography, Dona Paula, Goa, India

<sup>4</sup>Center of Advanced Study in Marine Biology, Annamalai University, Parangipettai, Tamil Nadu, India

<sup>5</sup>Laboratory for Protein Phosphorylation and Proteomics, O&N1 Herestraat 49, Box 901, 3000 Leuven, Belgium

\***Running title:** *Structure-function elucidation of a new  $\alpha$ -conotoxin*

To whom correspondence should be addressed: Jan Tytgat, Department of Pharmacy, Toxicology and Pharmacology, KU Leuven, Herestraat 49, 3000 Leuven, Belgium, Tel: +32 16 32 34 04; Fax: +32 16 32 34 05; Email: [jan.tytgat@pharm.kuleuven.be](mailto:jan.tytgat@pharm.kuleuven.be).

**Keywords:** conotoxin; nicotinic acetylcholine receptor; electrophysiology; NMR; protein engineering; Alzheimer's disease; schizophrenia; conotoxin structure-function relationship

**Background:**  $\alpha$ -Conotoxins are small toxins found produced by Cone snails and potent antagonists of nicotinic acetylcholine receptors.

**Results:** Two mutants were created to investigate the unusual C-terminus of a novel  $\alpha$ -conotoxin from *Conus longurionis*.

**Conclusions:** We characterized an important residue for discrimination between neuronal and muscle subtype nicotinic acetylcholine receptors.

**Significance:** This opens perspectives for designing new ligands to affect brain disorders.

### ABSTRACT

$\alpha$ -Conotoxins are small peptide toxins found in the venom of marine Cone snails and potent antagonists of various subtypes of nicotinic acetylcholine receptors (nAChRs). nAChRs are cholinergic receptors forming ligand-gated ion channels in the plasma membranes of certain neurons and the neuromuscular junction. As nAChRs have an important role in regulating transmitter release, cell excitability, and neuronal integration, nAChR dysfunctions have been implicated in a variety of severe pathologies such as epilepsy, myasthenic syndromes, schizophrenia, Parkinson's and Alzheimer's diseases.

In order to expand the knowledge concerning Cone snail toxins, we examined the venom of *Conus longurionis*. We isolated

an 18-amino acid peptide named  $\alpha$ -conotoxin Lo1a, which is active on nAChRs. To the best of our knowledge, this is the first characterization of a conotoxin from this species. The peptide was characterized by electrophysiological screening against several types of cloned nAChRs expressed in *Xenopus laevis* oocytes. The three-dimensional solution structure of the  $\alpha$ -conotoxin Lo1a was determined by NMR spectroscopy. Lo1a, member of the  $\alpha 4/7$  family, blocks the response to acetylcholine in oocytes expressing  $\alpha 7$  nAChRs with an  $IC_{50}$  of  $3.24 \pm 0.7 \mu M$ . Furthermore, Lo1a shows a high selectivity for neuronal versus muscle subtype nAChRs. As Lo1a has an unusual C-terminus, we designed two mutants, Lo1a- $\Delta D$  and Lo1a-RRR, in order to investigate the influence of the C-terminal residue. Lo1a- $\Delta D$  has a C-terminal Asp-deletion whereas in Lo1a-RRR, a triple Arg-tail replaces the Asp. They block  $\alpha 7$  with a lower  $IC_{50}$ -value, but remarkably, both shift the efficacy on the muscle subtype nAChR  $\alpha 1\beta 1\gamma \epsilon$ .

Nicotinic acetylcholine receptors (nAChRs) are expressed in the central and peripheral nervous systems where they are involved in many neuronal functions. These neuronal functions include differentiation and synaptic plasticity, which are the basis for learning and memory (1-3). The nicotinic

acetylcholine receptor family is classified into two subtypes based on their primary sites of expression, namely neuronal and muscle subtype nAChRs. Both subtypes are pentameric integral membrane protein complexes classified as ligand-gated ion channels that open in response to binding of the neurotransmitter acetylcholine (ACh) (4,5). The neuronal subtype nAChRs can include only  $\alpha$ -subunits like for instance  $\alpha_7$ ,  $\alpha_8$  and  $\alpha_9$ , called homomeric ion channels or they can combine two or more types of subunits, called heteromeric species. These heteromeric species are compiled of at least one  $\alpha$  ( $\alpha_2$ - $\alpha_{10}$ ) and one  $\beta$  ( $\beta_2$ - $\beta_4$ ) subunit. On the other hand, the muscle subtype nAChRs are composed of four different types of subunits ( $\alpha_1$ ,  $\beta_1$ ,  $\delta$ ,  $\epsilon/\gamma$ ) (6-8).

One of the neuronal nAChRs,  $\alpha_7$ , has received much attention since its discovery thanks to its role in the central nervous system (CNS) (9). This interest is because of the fact that the  $\alpha_7$  subunit is highly distributed in the brain, including regions involved in learning and memory, hippocampus and cerebral cortex (10-12). Consequently, nAChR dysfunctions have been implicated in a variety of severe pathologies like for instance certain types of epilepsy, myasthenic syndromes, schizophrenia, Parkinson's and Alzheimer's diseases (13-15). Therefore, the discovery of new ligands binding with high affinity and selectivity to nAChR subtypes is of prime interest in order to study these receptors and to potentially discover new drugs for the treatment of these pathologies (16).

One of the possibilities to find new ligands can be found in Cone snail species, from which the so called family of  $\alpha$ -conotoxins is a group of potent nAChRs antagonists (17,18). These  $\alpha$ -conotoxins are a series of structurally and functionally related peptides found in the venom of cone snail species. They are classified into subfamilies based on the number of residues in their two 'loops' between conserved Cys residues, with 3/5 (CCX<sub>3</sub>CX<sub>5</sub>C), 4/3 (CCX<sub>4</sub>CX<sub>3</sub>C) and 4/7 (CCX<sub>4</sub>CX<sub>7</sub>C) subfamilies the most common (19). The toxins of *Conus* sp. are usually potent, selective and small (12-25 amino acids) which is an advantage for cost-effective synthesis (20). Moreover, they are shown to function as specific probes to investigate structure-function relationship of nAChRs (17).

In this study, we report the isolation of a novel 18-amino acid  $\alpha$ -conotoxin from the venom of the marine snail *Conus longurionis* and its electrophysiological screening against six

different types of nAChRs. To the best of our knowledge, this is the first conotoxin to be characterized from this species found in the Indian Ocean in Tamil Nadu, India. The peptide, called Lola, has a "W-shape" structural conformation having two loops that are reinforced by two disulfide bonds. The function of the peptide was investigated by electrophysiological screenings and revealed that Lola was most active against neuronal homomeric  $\alpha_7$  nAChRs. To further determine structure-function relationship of Lola and its target  $\alpha_7$ , we engineered two synthetic analogues, namely Lola- $\Delta$ D and Lola-RRR, based on the protein sequence of Lola and its homology to other conotoxins from the  $\alpha$ 4/7 family. The first peptide, Lola- $\Delta$ D, has an Asp deletion at the C-terminus while in the second peptide an Arg-tail replaces this Asp. Both analogues are found to block  $\alpha_7$  with a lower IC<sub>50</sub>, but remarkably, there is a shift in efficacy on the muscle subtype nAChR  $\alpha_1\beta_1\delta\epsilon$ . These results reveal unexpected roles for the C-terminus in determining subtype selectivity and efficacy. As a consequence, our findings might be relevant in the context of designing novel therapeutic compounds with potential utility in diseases such as Alzheimer's disease, schizophrenia, and attention deficit hyperactivity disorder (ADHD), because as previously mentioned,  $\alpha_7$  nAChRs are thought to play important roles in the brain (21).

## EXPERIMENTAL PROCEDURES

*Cone snail specimens and venom extraction* – Specimens of *C. longurionis* (identified by Kiener in 1845 and classified by Tucker and Tenorio (22)) were collected from the Indian Ocean in Tamil Nadu, India. The venomous apparatuses (venom bulbs and venom ducts) were extracted from the specimens as previously described (23). The collected tissue was preserved in RNAlater solution (Ambion) and stored at -20 °C. The venomous apparatuses were used for total RNA extraction and peptide/protein extraction

*Peptide Fractionation and Purification* – Sample fractionation occurred by a reversed-phase HPLC system (Gilson). Two steps were followed for the separation of the venom compounds. In the first step, the lyophilized crude venom powder was solubilized into 50% ACN/water and aliquots were loaded on a Gel filtration Superdex™ Peptide 10/300 GL column with 50% ACN/water as mobile phase (flow rate 0.5 ml/min) to separate the peptides and proteins

based on their size. Two sample collections were made that were stored overnight at  $-80^{\circ}\text{C}$ , freeze-dried and finally solubilized in 5% ACN/water. For the second step, an analytical Vydac C<sub>18</sub> column (218MS54, 4.6 x 250 mm, 5- $\mu\text{m}$  particle size; Grace, Deerfield, IL) with a two solvent system was used: (A) 0.1% trifluoroacetic acid (TFA)/H<sub>2</sub>O and (B) 0.085% TFA/Acetonitrile (ACN). The sample was eluted at a constant flow rate of  $1\text{ml}\cdot\text{min}^{-1}$  with a 0-80% gradient of solvent B over 90 min (1% ACN per minute after 10 minutes of solvent A). The HPLC column elutes were monitored by a UV/VIS-155 detector (Gilson) scanning both 214 nm and 280 nm.

*Peptide Sequencing* – Isolated Lol1a was collected and freeze-dried for direct peptide sequencing and molecular mass analysis (MALDI-TOF). A Protein Sequencer PPSQ-31A/33A (Shimadzu, Japan) was used to determine the amino acid sequence of the separated compound. In this Edman degradation method, the sample was loaded onto a polybrene-pretreated, precycled glass fibre disk, and Edman sequenced for 24 residue cycles.

*Peptide synthesis and folding* – Lol1a was synthesized using Fmoc chemistry by GeneCust (Luxemburg). Lol1a- $\Delta\text{D}$  and Lol1a-RRR were synthesized by GenicBio Limited (Shanghai, China). Formation of the two disulfide bridges was carried out by adopting the selective protection and de-protection strategy in vitro. The resulting bicyclic peptides were subsequently purified by HPLC and analyzed with ESI-MS, then freeze-dried and stored at  $-20^{\circ}\text{C}$  until use.

*Functional characterization* – Complementary DNA encoding the nAChR-channels was subcloned into the corresponding vector: human  $\alpha_3$ /pcDNA3(XbaI), human  $\alpha_4$ /pGEM-HE(NheI), chick  $\alpha_7$ /pBlueScript(NotI), human  $\beta_2$ /pSP64(PvuII), human  $\beta_4$ /pcDNA3(XbaI), rat  $\alpha_1$ /pSP0oD(SalI), rat  $\beta_1$ /pSP0oD(SalI), rat  $\gamma$ /pSP0oD(SalI), rat  $\delta$ /pSP0oD(SalI), rat  $\epsilon$ /pSP0oD(SalI). The linearized plasmids - respective restriction enzymes are indicated in parentheses - were transcribed using the T7 ( $\alpha_3$ ,  $\alpha_4$ ,  $\alpha_7$ ,  $\beta_4$ ) or the SP6 ( $\beta_2$ ,  $\alpha_1$ ,  $\beta_1$ ,  $\gamma$ ,  $\delta$ ,  $\epsilon$ ) mMACHINE transcription kit (Ambion, Austin, TX).

The harvesting of stage V-VI oocytes from anaesthetized female *Xenopus laevis* frogs was previously described (24). Oocytes were injected with 50-70 nl of cRNA at a

concentration of 1-3 ng/nl using a micro-injector (Drummond Scientific, Broomall, PA). The oocytes were incubated in a ND-96 solution containing: 96 mM NaCl, 2 mM KCl, 1.8 mM CaCl<sub>2</sub>, 2 mM MgCl<sub>2</sub> and 5 mM HEPES (pH 7.4), supplemented with 1.25 ml/l gentamycin and 90 mg/l theophyllin. Oocytes were stored for 1-5 days at  $16^{\circ}\text{C}$  until sufficient expression of nAChRs was achieved.

Whole-cell currents from oocytes were recorded at room temperature ( $18-22^{\circ}\text{C}$ ) by the two-electrode voltage clamp technique using a GeneClamp 500 amplifier (Molecular Devices, Sunnyvale, CA) controlled by a pClamp data acquisition system (Molecular Devices). Oocytes were placed in a bath containing ND-96 solution. Voltage and current electrodes were filled with 3M KCl, and the resistances of both electrodes were between 0.5 and 1.5 M $\Omega$ . The elicited currents were sampled at 100 Hz and filtered at 50 Hz using a four-pole, low pass Bessel filter. To eliminate the effect of the voltage drop across the bath grounding electrode, the bath potential was actively controlled by a two-electrode bath clamp. During recordings, oocytes were continuously perfused with ND96-A (ND96 with 1  $\mu\text{M}$  atropine; except for  $\alpha_7$ ) at a rate of 2 mL/min, with the conopeptides applied during 30s before ACh was added. ACh (200  $\mu\text{M}$  for  $\alpha_7$ , 70  $\mu\text{M}$  for  $\alpha_3\beta_4$ , 50  $\mu\text{M}$  for  $\alpha_4\beta_2$  and  $\alpha_4\beta_4$ , 10  $\mu\text{M}$  for  $\alpha_1\beta_1\gamma\delta$  and  $\alpha_1\beta_1\gamma\epsilon$ ) was applied for 2s at 2 mL/min, with 30s washout periods between different ACh applications and 200s after toxin application. The percentage response or percentage inhibition was obtained by averaging the peak amplitude of three control responses (two directly before exposure to the peptide and one after 200s washout).

Whole-cell current traces were evoked from a holding potential of  $-90\text{ mV}$ . Concentration-response curves were constructed by application of different toxin concentrations to the nAChR-expressing oocytes. The percentage of nAChR-blockade was plotted against the logarithm of the applied concentrations and fitted with the Hill equation:  $y = 100/[1 + (EC_{50}/[\text{toxin}]^h]$ , where  $y$  is the amplitude of the toxin-induced effect,  $EC_{50}$  is the toxin concentration at half maximal efficacy,  $[\text{toxin}]$  is the toxin concentration and  $h$  is the Hill coefficient.

Comparison of two sample means was made using a paired Student's  $t$  test ( $p < 0.05$ ). All data are presented as mean  $\pm$  standard error (S.E.M) of at least 3 independent experiments ( $n \geq 3$ ). All

data was analyzed using pClamp Clampfit 10.0 (Molecular Devices®, Downingtown, PA) and Origin 7.5 software (Originlab®, Northampton, MA).

*NMR Spectroscopy* – NMR spectra were recorded with a 2.6 mM solution (200  $\mu$ L, pH 5.9) of the folded conopeptide in D<sub>2</sub>O and in H<sub>2</sub>O:D<sub>2</sub>O (9:1) mixture at 5 °C on a 600 MHz Bruker Avance II spectrometer equipped with a 5mm TCI HCN Z-gradient cryoprobe. Spectra were processed using Topspin 2.1 (Bruker Biospin) and analyzed by using CARA program (version 1.8.4) (25).

In the one-dimensional and two-dimensional spectra that were recorded in H<sub>2</sub>O:D<sub>2</sub>O mixture, the water signal was suppressed by using excitation sculpting with gradients (26). The two-dimensional NOESY in H<sub>2</sub>O (mixing time 150 and 300 ms) was recorded with a sweep width of 7210 Hz in both dimensions, 64 scans, 2048 data points in  $t_2$ , and 1024 free induction decays (FIDs) in  $t_1$ .

A two-dimensional total correlation spectroscopy (2D-TOCSY) (27) in 90% H<sub>2</sub>O was recorded with DIPSI2 sequence for mixing (mixing time 80 ms). A double quantum-filtered correlation spectrum (DQF-COSY) (28) in H<sub>2</sub>O was acquired using excitation sculpting with gradients for water suppression with a sweep width of 7210 Hz in both dimensions, 64 scans, 2048 data points in  $t_2$ , and 1024 FIDs in  $t_1$ . In the processing of two-dimensional spectra the data were apodized with a shifted sine-bell square function in both dimensions. Proton chemical shifts were calibrated by using residual HOD signal as reference (4.9745 ppm at 5 °C).

Natural abundance <sup>1</sup>H, <sup>13</sup>C heteronuclear single quantum correlation (<sup>1</sup>H-<sup>13</sup>C HSQC) spectrum in D<sub>2</sub>O was recorded with sensitivity enhancement and gradient coherence selection optimized for selection of aliphatic CH groups ( $J_{CH} = 135$  Hz) using 64 scans, 1024/2048 complex data points, and 12072/7210 Hz spectral widths in  $t_1$  and  $t_2$  respectively. For the selection of aromatic CH groups 170 Hz was used for  $J_{CH}$  along with 32 scans, and 64/2048 complex data points. The two-dimensional heteronuclear single quantum correlation-total correlation spectroscopy (HSQC-TOCSY) spectrum was recorded with a pulse program consisted of an HSQC building block followed by a clean MLEV-17 TOCSY transfer step of 80 ms mixing time just prior to the refocusing gradients with exactly the same spectral widths

and number of points as in the aliphatic <sup>1</sup>H-<sup>13</sup>C HSQC.

Distance restraints were derived from cross-peak volumes of the NOESY spectrum recorded with 150 ms mixing time. Estimated interproton distances were derived using the isolated spin pair approximation,  $r_{ij} = r_{ref} (v_{ref}/v_{ij})^{1/6}$  where  $r_{ij}$  is the estimated interproton distance,  $r_{ref}$  is the fixed internal reference distance, and  $v_{ref}$  and  $v_{ij}$  are the NOE cross-peak volumes of the reference and estimated cross-peaks respectively. Average cross-peak volume of the geminal methylene proton pairs was used as reference volume which corresponds to the fixed reference distance of 1.8 Å. Generally an experimental error of  $\pm 20\%$  on the calculated interproton distances was used as upper and lower bounds. The <sup>3</sup> $J_{HNH\alpha}$  coupling constants were measured from the one-dimensional proton spectrum recorded in H<sub>2</sub>O and then converted to dihedral restraints as follows: <sup>3</sup> $J_{HNH\alpha} > 8$  Hz,  $\varphi = -120 \pm 30^\circ$ ; <sup>3</sup> $J_{HNH\alpha} < 6$  Hz;  $\varphi = -60 \pm 30^\circ$ ;  $\omega = 180 \pm 30^\circ$  to define the trans X-Pro<sup>7/14</sup> conformation as confirmed by the observation of strong NOE interactions between Ha( $n$ ) and HD2, HD3 ( $n+1$ ) Pro.

All structure calculations were performed by using Xplor-NIH program, version 2.25 (29). A set of 100 structures was generated by torsion angle molecular dynamics, starting from an extended strand and by using NMR-derived restraints. After the torsion angle molecular dynamics round (30), the majority of the structures had converged to very similar structures with similar total energies and having no violations of the NOE and dihedral restraints. Fifteen lowest energy structures were used for further refinement during a “gentle molecular dynamics” round in explicit water (31). A box of water was constructed and optimized around selected structures obtained from the previous torsion angle dynamics step. The final stage of refinement commenced with a 20 ps constant temperature molecular dynamics simulation at 300K (20,000 steps of 0.001 ps) and was followed by a 200-step conjugate gradient energy minimization of the average structure of the last 10 ps of the 20 ps simulation. Structures were analyzed by using PROCHECK (32). Visual representations of the molecule were created by using UCSF Chimera program (version 1.8rc).

## RESULTS

*Isolation of a novel  $\alpha$ -conotoxin from *C. longurionis* venom* – N-terminal Edman degradation of the purified active peptide revealed a novel 18-residue  $\alpha$ -conotoxin, called Lol1a, with the sequence H-EGCCSNPACRTNHPEVCD-NH<sub>2</sub> (bridges Cys<sup>3</sup>-Cys<sup>9</sup> and Cys<sup>4</sup>-Cys<sup>17</sup>) and a molecular mass of 1930.12 Da, determined by MALDI-TOF (4800 Analyzer, Applied Biosystems, USA). To the best of our knowledge, Lol1a is the first conotoxin isolated and pharmacologically characterized from *C. longurionis*, a species of a (vermivorous) cone snail commonly found in the Indian Ocean in Tamil Nadu, India. It has highest sequence homology with Qc1.5 (81%, Table 1), which is isolated from *C. quercinus*, another vermivorous cone snail (33).

*$\alpha$ -Conotoxin Lol1a analogues* – Typically,  $\alpha$ -conotoxins end C-terminally with a Cys (see Table 1). Interestingly, Lol1a ends with an Asp following this Cys. Only two more conotoxins having an Asp at the C-terminus are described, namely Lp1.4 (34) and Bt1.91. To explore the influence of the C-terminal Asp-18 to the functional properties of Lol1a, we created two synthetic analogues: Lol1a- $\Delta$ D and Lol1a-RRR. The synthetic analogues Lol1a- $\Delta$ D (molecular mass 1815.03 Da) is C-terminally truncated whereas in Lol1a-RRR (molecular mass 2283.60 Da) the negatively charged Asp is replaced by a positive charged Arg-tail.

*Lol1a inhibition of recombinant nAChR subtypes* – The potency and selectivity of Lol1a at neuronal nAChRs was determined by examining its effect on ACh-evoked currents mediated by different nAChR subunit combinations expressed in *Xenopus* oocytes. Lol1a (10  $\mu$ M) inhibited ACh-evoked current amplitude mediated by  $\alpha_7$  (85%),  $\alpha_3\beta_4$  (40%),  $\alpha_4\beta_2$  (17%),  $\alpha_4\beta_4$  (13%) (Figure 1). No remarkable effect was seen at the muscle subtype nAChRs  $\alpha_1\beta_1\gamma\delta$  and  $\alpha_1\beta_1\delta\epsilon$  (for concentrations up to 50  $\mu$ M). Concentration-response curves for Lol1a inhibition of ACh-evoked currents at the  $\alpha_7$  nAChR revealed an IC<sub>50</sub>-value of  $3.24 \pm 0.70$   $\mu$ M (Figure 2).

*Influence of C-terminal truncation and replacement of -D by -RRR* – We synthesized a C-terminally truncated analogue of Lol1a to examine its activity at different nAChR subtypes (Figures 3 and 4). Interestingly, Lol1a- $\Delta$ D was more potent at the  $\alpha_7$ -subtype (IC<sub>50</sub> =  $0.80 \pm 0.01$  nM) but surprisingly also gained activity on the muscle subtype nAChR  $\alpha_1\beta_1\delta\epsilon$  (IC<sub>50</sub> =  $4.40 \pm$

0.18  $\mu$ M) (Figure 5). The same was noticed for Lol1a-RRR where the IC<sub>50</sub> for  $\alpha_7$  was 1.06  $\mu$ M and an IC<sub>50</sub>-value of  $1.47 \pm 0.39$   $\mu$ M was determined for  $\alpha_1\beta_1\delta\epsilon$  (Figure 5). An overview of subtype selectivity for Lol1a and both mutants is given in Figure 6.

*NMR spectroscopy* – NMR spectral analysis shows the formation of a single set of resonances for the conopeptide, indicating that it adopts one type of structural form in solution. Resonance assignment was performed by following standard procedures as outlined by Wüthrich and co-workers (35). Complete sequence specific proton assignments were achieved by analyzing homo-nuclear two-dimensional (2D) spectra (DQF-COSY, TOCSY, and NOESY). Initially the NH and Ha resonances of the individual spin systems (except Pro) were identified by analyzing the so-called “fingerprint” region of the DQF-COSY and TOCSY spectra and the remaining resonances of the spin systems were identified by following the so-called “TOCSY-tower”. Sequence specific assignments were achieved by linking individual spin system via sequential inter-residue *Han*-HN(*n+1*) cross-peaks in the “fingerprint” region of the NOESY spectrum. Carbon assignments were also performed by using <sup>1</sup>H-<sup>13</sup>C HSQC spectra, which further reconfirmed most of the homo-nuclear proton assignments and clarified the H $\beta$  and H $\gamma$  proton assignments of the two proline residues that were not resolved in the homo-nuclear 2D spectra due to signal overlaps. The geminal methylene protons were not assigned stereo-specifically and the NOE distance restraints involving these protons were used ambiguously during structure calculation in the Xplor-NIH program. Figure 7 shows the observed short and medium range NOEs that were used for the resonance assignment, <sup>3</sup>J<sub>HNH $\alpha$</sub> , and chemical shift index (CSI) along the amino acid sequences of  $\alpha$ -conotoxin Lol1a. The CSI values indicate the presence of an  $\alpha$ -helix in the middle of the peptide from residue Pro<sup>7</sup> to Asn<sup>12</sup>.

Figure 8 displays the structural representations of the final ensemble of 15 superimposed structures (Figure 8A) and the minimum-energy closest-to-average structure (Figure 8B) of  $\alpha$ -conotoxin Lol1a. The peptide structures are well defined with backbone and heavy atom RMSD of 0.43 and 0.83 respectively over residues 3 to 17. The structural evaluation using PROCHECK demonstrates that all the resulted structures are having no bad non-bonded contacts and all the backbone dihedral angles are

within the allowed regions of the Ramachandran plot (63% residues fall in the most favored region). Detailed structure determination statistics are provided in Table 1. The coordinates for 15 structures, NMR restraints and chemical shifts have been deposited in the RCSB Protein Data Bank with RCSB ID RCSB Lo1a and PDB ID Lo1a (to be deposited).

A close look into the structure (Figure 8 ) of the  $\alpha$ -conotoxin Lo1a reveals that the peptide backbone adopts a compact “W-shaped” conformation having two loops that are reinforced by two disulfide bonds (Cys<sup>3</sup>-Cys<sup>9</sup> and Cys<sup>4</sup>-Cys<sup>17</sup>). Residues from Pro<sup>7</sup> to Asn<sup>12</sup> at the bottom of the “W-shape” formed an  $\alpha$ -helix involving two-turns. Besides this, in the N-terminal part of the peptide structure two overlapping beta-turns (type IV) exist between Gly<sup>2</sup> to Ser<sup>5</sup> and Cys<sup>4</sup> to Pro<sup>7</sup>. In the C-terminal part of the peptide, residues from Pro<sup>14</sup> to Cys<sup>17</sup> formed a type I/IV beta-turn. This type of overall “W-shaped” molecular topology/fold was previously identified in the reported structures of other  $\alpha$ 4/7 subfamily  $\alpha$ -conotoxins (36,37).

## DISCUSSION

Alpha-conotoxins are a family of cysteine-rich peptides that behave pharmacologically as competitive antagonists of the nicotinic acetylcholine receptor (38). In general, there are two main nAChR subtypes, the neuronal and muscle subtype nAChRs. Considering the **neuronal subtype nAChRs** and particularly their ACh binding site, a high percentage of sequence identity exists among the known neuronal nAChR subunits (39,40). Due to the high sequence conservation, it has been difficult to obtain subtype selective ligands, principally agonists that take action deep within the conserved ACh binding pocket. However recently, selective peptide antagonists from cone snail venom have shown to be highly selective pharmacological tools having the ability to discriminate amongst many of the different nAChR subunit combinations (40). This high selectivity toward a particular mammalian nAChR subtype is often established through specific interaction with particular residues located outside the conserved ACh binding site (41). Nowadays, co-crystal structures of  $\alpha$ -conotoxins binding to the acetylcholine binding protein (AChBP) (42), which is a protein model for the extracellular ligand-binding domain of nAChRs, can offer useful information about the

molecular interactions of these small peptides (43,44).

*Lo1a has a typical  $\alpha$ -conotoxin structure* – In our study we revealed the amino acid composition and the 3-dimensional structure of a new  $\alpha$ 4/7-conotoxin from *Conus longurionis*, called Lo1a. The peptide was investigated electrophysiologically and the results show that Lo1a inhibits  $\alpha_7$  nAChRs preferentially. Once the activity of Lo1a had been determined we employed NMR based techniques to elucidate the structure of this novel peptide. According to Marx (45), NMR is the method of choice for determining conotoxin structures, because conotoxins are generally difficult to crystallize, and are not amenable to X-ray methods, with a few exceptions such as PnIA and PnIB (46,47).  $\alpha$ -Conotoxin Lo1a showed to be highly soluble and NMR spectra were readily assigned and used to generate a high-resolution structure. This structure shows that Lo1a shares many of the structural and biochemical properties that define  $\alpha$ -conotoxins, including the characteristic I-III, II-IV disulfide connectivity and the size of the first and the second loop of the peptide, i.e. four and seven residues respectively. Several  $\alpha$ -conotoxins including AnIB (48), OmIA (49), GID (50), RegIIA (51) and LsIA (52) have an SXPA motif similar to the first loop of Lo1a. The peptide also shares the common fold comprising a short disulfide bond stabilized helix and a conserved proline. This proline is shown to be the only highly conserved amino acid residue apart from the cysteines and is responsible for helix initiation by inducing the  $3_{10}$  helix turn in the peptide backbone (38). Dutertre and Lewis (2006) revealed that this small  $\alpha$ -helix structure appears to be a very important determinant for binding, even if the orientations and specific interactions differ significantly. As the side chains in an  $\alpha$ -helix protrude at  $360^\circ$ , this structure is likely suitable to allow multiple contacts on both sides of a binding pocket located at the interface of two subunits (38).

*Lo1a has an atypical C-terminus* – The N-terminal amino acid residue of  $\alpha$ -conotoxins is typically a glycine followed by the first two cysteine residues (Table 1). However, sequence alignment of Lo1a with other  $\alpha$ -conotoxins reveals besides a unique loop-2 sequence an atypical terminal amino acid sequence as both N- and C-termini contain negatively charged amino acid residues, i.e. glutamic acid and aspartic acid respectively. Few conotoxins have other residues preceding the first cysteine. From these

conotoxins, ArIA (53), ArIB (53), GID (50), PIA (54), EI (55) and LsIA (52) are the most investigated (Table 1). On the other hand, a negative residue at the C-terminus of an  $\alpha$ -conotoxin has only been observed in conotoxins Lp1.4 from *Conus leopardus* (33) and Bt1.91 from *Conus betulinus*. But to the best of our knowledge, the influence of this negative C-terminal residue has never been investigated before.

*C-terminal charges reveal to be important for neuronal/muscle subtype selectivity and efficacy* – To explore the role of the C-terminal Asp of Lo1a, two analogues were synthesized: one C-terminally truncated peptide, named Lo1a- $\Delta$ D and another named Lo1a-RRR with an extremely positively charged Arg-tail at the C-terminus. Deleting the C-terminal amino acid resulted in a more positively charged peptide, while the rationale for the Arg-tailing peptide can be found in the sequences of ArIA and ArIB (Table 1) from *C. arenatus*. Both peptides, ArIA and ArIB, are potent inhibitors of the  $\alpha_7$  nAChR having IC<sub>50</sub>-values in the nanomolar range (53). Whiteaker et al. (2007) made a series of directed substitutions in ArIB to obtain a more selective  $\alpha_7$  antagonist. The mutant ArIB[V11L,V16D] improved its selectivity on  $\alpha_7$  more than 10.000 fold suggesting the importance of Lys and Asp on position 11 and 16 respectively. Via replacing the C-terminal Asp by a triple Arg-tail, we aimed to investigate whether we could improve potency/selectivity on  $\alpha_7$  with Lo1a-RRR.

The two synthetic C-terminal modified analogues revealed unexpected roles for the C-terminus in determining subtype selectivity and efficacy. Both mutants demonstrate more potency towards the neuronal  $\alpha_7$  AChR as both IC<sub>50</sub> values decreased from 3.24  $\mu$ M (Lo1a) to 0.80  $\mu$ M (Lo1a- $\Delta$ D) and 1.06  $\mu$ M (Lo1a-RRR). As the difference in potency is not very astonishing, we can conclude that the C-terminal residue(s) doesn't play a crucial role in activity on  $\alpha_7$ . Remarkably, both mutants influence the efficacy of the adult muscle subtype AChR  $\alpha_1\beta_1\delta\epsilon$  (IC<sub>50</sub> values  $4.40 \pm 0.18$   $\mu$ M (Lo1a- $\Delta$ D) and  $1.47 \pm 0.39$   $\mu$ M (Lo1a-RRR)) but not on the fetal muscle subtype AChR  $\alpha_1\beta_1\gamma\delta$ . Consequently, C-terminal charges seem to have an influence in making the distinction between neuronal or muscle subtype nAChRs and even among muscle subtype nAChRs.

Typically  $\alpha$ -conotoxins that target selectively muscle subtype nAChRs have a 3/5 structure (56). An exception is the  $\alpha$ -conotoxin EI ( $\alpha_4/7$ )

from *C. ermineus* that selectively targets the  $\alpha/\delta$  interface of muscle subtype nAChRs (55). Conotoxins that distinguish between the adult en the fetal muscle subtype nAChRs are rather rare. One example is  $\psi$ -conotoxin PrIIIE from *C. parvus*, characterized by Luisma et al. (2008), which showed higher inhibition potency against the adult subtype (IC<sub>50</sub> of 245 nM) than the fetal-subtype nAChR (IC<sub>50</sub> of 3.24  $\mu$ M) (57). Another  $\psi$ -conotoxin PIIIE from *C. purpurascens* shows an IC<sub>50</sub> of 7.4  $\mu$ M on the adult muscle subtype, but no inhibition on the fetal muscle subtype for concentrations up to 10  $\mu$ M. Teichert et al. (2005) reports a  $\alpha$ A-conotoxin OIVB from *C. obscurus*, a unique selective inhibitor of the mammalian fetal muscle nAChR (IC<sub>50</sub> of 56 nM), whereas affinity for the adult muscle nAChR is more than 1800-fold lower (58). According to Groebe et al. (1995), many of the  $\alpha$ -conotoxins bind with 10.000-fold higher affinity to the mammalian  $\alpha/\delta$  interface than the  $\alpha/\gamma$  interface (59). Our mutants, Lo1a- $\Delta$ D and Lo1a-RRR apparently demonstrate higher affinity to the  $\alpha/\epsilon$  interface.

If we consider the terminal charges of Lo1a and its analogue, we expect that the positively charged triple Arg-tail in Lo1a-RRR is more likely to adapt a conformation extended away from the negatively charged N-terminus (as derived by torsion-angle molecular dynamics and energy minimization in the structural model). In contrast, the structure from Lo1a has a more 'compact' conformation, with an inward-facing C-terminus as derived from the solution state NMR structural data. Consequently, as the C- and N-terminus of Lo1a are into close distance (less than 10 nanometer), the charges at both termini may interact, playing a role in making the distinction between neuronal versus muscle subtype nAChRs. Further structure-function studies combined with co-crystallization experiments are necessary to see whether this hypothesis is applicable for Lo1a- $\Delta$ D.

*Muscle and neuronal subtype nAChRs binding sites: structural receptor elements for binding of Lo1a and its homologous* – **The muscle subtype nAChR** has a pentameric structure comprised of two  $\alpha_1$  subunits, one  $\beta_1$ , one  $\delta$ , and depending on whether the receptor is in an embryonic or adult stage, one  $\gamma$  or  $\epsilon$  subunit respectively. Each  $\alpha_1$ -subunit folds such that the primary binding site directly faces a neighboring subunit, which is either a  $\gamma/\epsilon$  or a  $\delta$ -subunit. The  $\gamma$ -subunit is believed to be the one that forms stable contacts being the lone subunit between

the two  $\alpha$ -subunits, while the  $\delta$ -subunit pairs with the  $\beta$ -subunit to form stable contacts between the  $\alpha$ -subunits on the opposite side (Figure 9). As two  $\alpha_1$ -subunits are separated by at least one non  $\alpha$ -subunit, correct coupling between these subunits is required for cooperative binding of agonists (60). Agonists of the muscle subtype nAChR initiate channel opening and desensitization by binding to a site on each of these two  $\alpha_1$  subunits (61). Moreover, Arias and Blanton (2000) established that two adjacent cysteines (at position 192 and 193 according to the sequence number of *Torpedo* AChR) in the  $\alpha_1$  subunits are involved in the recognition and binding of cholinergic agonists and competitive antagonists (19). Later on, Sine (1993) demonstrated that not only the two  $\alpha_1$ -subunits form the binding sites of agonists and antagonist, but that also the  $\gamma$ / $\epsilon$  and  $\delta$  subunits are involved (62). Agonists and antagonists can specifically distinguish between the  $\alpha_1\gamma$ / $(\alpha_1\epsilon)$  and  $\alpha_1\delta$  binding sites of the fetal/(adult) muscle acetylcholine receptor because of different contributions by the  $\gamma$ / $\epsilon$  and  $\delta$  subunits where a minimum of four loops in both subunits is required to create the agonist binding site (63). In 1991, Sine and Claudio showed that AChRs lacking either a  $\gamma$  or a  $\delta$  subunit assemble into pentamers with subunit compositions,  $(\alpha)_2\beta(\gamma)_2$  and  $(\alpha)_2\beta(\delta)_2$  (60). Therefore, we tried to express

$(\alpha)_2\beta(\gamma)_2$  and  $(\alpha)_2\beta(\delta)_2$  and  $(\alpha)_2\beta(\epsilon)_2$  heterologously to determine which binding site is responsible for interactions causing the observed results.

Whereas the two ligand binding sites of muscle AChRs are formed at interfaces between  $\alpha_1$  and  $\delta$ ,  $\epsilon$  or  $\gamma$  subunits, **binding sites of  $\alpha_7$  neuronal AChRs** are formed at interfaces between identical  $\alpha_7$  subunits. Residues of the  $\alpha$  face of the binding site, termed the (+) face, cluster in three well separated regions of the primary sequence, termed loops A, B, and C (63). The stabilization of this loop C conformation in an open state appears to be an essential element for antagonist activity. The stabilization in the AChBP is established on the basis of the loop C vicinal disulfide bonds where the  $\alpha$ -conotoxin disulfide bond Cys I-III interacts, as is shown for conotoxins PnIA and ImI (38). This type of antagonist activity can also be expected for Lo1a and its analogues, as both conotoxins, PnIA and ImI, are structurally quite homologous to Lo1a.

Our study provides insight into  $\alpha$ -conotoxin pharmacology and the molecular basis of nAChR selectivity, highlighting the influence and importance of C-terminal residues on conotoxin pharmacology.

## REFERENCES

1. Alberola-Die, A., Martinez-Pinna, J., Gonzalez-Ros, J. M., Ivorra, I., and Morales, A. (2011) Multiple inhibitory actions of lidocaine on *Torpedo* nicotinic acetylcholine receptors transplanted to *Xenopus* oocytes. *J Neurochem* **117**, 1009-1019
2. Gold, A. B., and Lerman, C. (2012) Pharmacogenetics of smoking cessation: role of nicotine target and metabolism genes. *Hum Genet*
3. Rezvani, A. H., and Levin, E. D. (2001) Cognitive effects of nicotine. *Biol Psychiatry* **49**, 258-267
4. Cooper, E., Couturier, S., and Ballivet, M. (1991) Pentameric structure and subunit stoichiometry of a neuronal nicotinic acetylcholine receptor. *Nature* **350**, 235-238
5. Insera, M. C., Kompella, S. N., Vetter, I., Brust, A., Daly, N. L., Cuny, H., Craik, D. J., Alewood, P. F., Adams, D. J., and Lewis, R. J. (2013) Isolation and characterization of alpha-conotoxin LsIA with potent activity at nicotinic acetylcholine receptors. *Biochem Pharmacol*
6. Colquhoun, L. M., and Patrick, J. W. (1997) Pharmacology of neuronal nicotinic acetylcholine receptor subtypes. *Adv Pharmacol* **39**, 191-220
7. Le Novere, N., and Changeux, J. P. (1995) Molecular evolution of the nicotinic acetylcholine receptor: an example of multigene family in excitable cells. *J Mol Evol* **40**, 155-172
8. Gotti, C., Fornasari, D., and Clementi, F. (1997) Human neuronal nicotinic receptors. *Prog Neurobiol* **53**, 199-237
9. Couturier, S., Bertrand, D., Matter, J. M., Hernandez, M. C., Bertrand, S., Millar, N., Valera, S., Barkas, T., and Ballivet, M. (1990) A neuronal nicotinic acetylcholine receptor subunit (alpha 7) is developmentally regulated and forms a homo-oligomeric channel blocked by alpha-BTX. *Neuron* **5**, 847-856



10. Rubboli, F., Court, J. A., Sala, C., Morris, C., Chini, B., Perry, E., and Clementi, F. (1994) Distribution of nicotinic receptors in the human hippocampus and thalamus. *Eur J Neurosci* **6**, 1596-1604
11. Wevers, A., Jeske, A., Lobron, C., Birtsch, C., Heinemann, S., Maelicke, A., Schroder, R., and Schroder, H. (1994) Cellular distribution of nicotinic acetylcholine receptor subunit mRNAs in the human cerebral cortex as revealed by non-isotopic in situ hybridization. *Brain Res Mol Brain Res* **25**, 122-128
12. Breese, C. R., Adams, C., Logel, J., Drebing, C., Rollins, Y., Barnhart, M., Sullivan, B., Demasters, B. K., Freedman, R., and Leonard, S. (1997) Comparison of the regional expression of nicotinic acetylcholine receptor alpha7 mRNA and [125I]-alpha-bungarotoxin binding in human postmortem brain. *J Comp Neurol* **387**, 385-398
13. Gotti, C., and Clementi, F. (2004) Neuronal nicotinic receptors: from structure to pathology. *Prog Neurobiol* **74**, 363-396
14. Sacco, K. A., Bannon, K. L., and George, T. P. (2004) Nicotinic receptor mechanisms and cognition in normal states and neuropsychiatric disorders. *J Psychopharmacol* **18**, 457-474
15. Steinlein, O. K., and Bertrand, D. (2010) Nicotinic receptor channelopathies and epilepsy. *Pflugers Arch* **460**, 495-503
16. Quinton, L., Servent, D., Girard, E., Molgo, J., Le Caer, J. P., Malosse, C., Haidar el, A., Lecoq, A., Gilles, N., and Chamot-Rooke, J. (2013) Identification and functional characterization of a novel alpha-conotoxin (EIIA) from *Conus ermineus*. *Anal Bioanal Chem* **405**, 5341-5351
17. Sine, S. M., Kreienkamp, H. J., Bren, N., Maeda, R., and Taylor, P. (1995) Molecular dissection of subunit interfaces in the acetylcholine receptor: identification of determinants of alpha-conotoxin M1 selectivity. *Neuron* **15**, 205-211
18. McIntosh, J. M., Plazas, P. V., Watkins, M., Gomez-Casati, M. E., Olivera, B. M., and Elgoyhen, A. B. (2005) A novel alpha-conotoxin, PeIA, cloned from *Conus pergrandis*, discriminates between rat alpha9alpha10 and alpha7 nicotinic cholinergic receptors. *J Biol Chem* **280**, 30107-30112
19. Arias, H. R., and Blanton, M. P. (2000) Alpha-conotoxins. *Int J Biochem Cell Biol* **32**, 1017-1028
20. Olivera, B. M., Rivier, J., Clark, C., Ramilo, C. A., Corpuz, G. P., Abogadie, F. C., Mena, E. E., Woodward, S. R., Hillyard, D. R., and Cruz, L. J. (1990) Diversity of *Conus* Neuropeptides. *Science* **249**, 257-263
21. Gronlien, J. H., Hakerud, M., Ween, H., Thorin-Hagene, K., Briggs, C. A., Gopalakrishnan, M., and Malysz, J. (2007) Distinct profiles of alpha7 nAChR positive allosteric modulation revealed by structurally diverse chemotypes. *Mol Pharmacol* **72**, 715-724
22. Tucker, J. K., and Tenorio, M. J. (2009) *Systematic Classification of Recent and Fossil Conoidean Gastropods: With Keys to the Genera of Cone Shells*, ConchBooks
23. Olivera, B. M., Gray, W. R., Zeikus, R., McIntosh, J. M., Varga, J., Rivier, J., de Santos, V., and Cruz, L. J. (1985) Peptide neurotoxins from fish-hunting cone snails. *Science* **230**, 1338-1343
24. Van Der Haegen, A., Peigneur, S., and Tytgat, J. (2011) Importance of position 8 in mu-conotoxin KIIIA for voltage-gated sodium channel selectivity. *FEBS J* **278**, 3408-3418
25. Keller, M., and Steiger, R. (2004) The pi plate: an implant for unstable extension fractures of the distal radius in patients with osteoporotic bone. *Tech Hand Up Extrem Surg* **8**, 212-218
26. Hwang, T. L., and Shaka, A. J. (1998) Multiple-pulse mixing sequences that selectively enhance chemical exchange or cross-relaxation peaks in high-resolution NMR spectra. *J Magn Reson* **135**, 280-287
27. Shaka, A. J., Lee, C. J., and Pines, A. (1988) Iterative Schemes for Bilinear Operators - Application to Spin Decoupling. *Journal of Magnetic Resonance* **77**, 274-293
28. Derome, A. E., and Williamson, M. P. (1990) Rapid-Pulsing Artifacts in Double-Quantum-Filtered Cosy. *Journal of Magnetic Resonance* **88**, 177-185
29. Schwieters, C. D., Kuszewski, J. J., Tjandra, N., and Clore, G. M. (2003) The Xplor-NIH NMR molecular structure determination package. *J Magn Reson* **160**, 65-73

30. Stein, E. G., Rice, L. M., and Brunger, A. T. (1997) Torsion-angle molecular dynamics as a new efficient tool for NMR structure calculation. *J Magn Reson* **124**, 154-164
31. Spronk, C. A., Linge, J. P., Hilbers, C. W., and Vuister, G. W. (2002) Improving the quality of protein structures derived by NMR spectroscopy. *J Biomol NMR* **22**, 281-289
32. Laskowski, R. A., Macarthur, M. W., Moss, D. S., and Thornton, J. M. (1993) Procheck - a Program to Check the Stereochemical Quality of Protein Structures. *J Appl Crystallogr* **26**, 283-291
33. Yuan, D. D., Han, Y. H., Wang, C. G., and Chi, C. W. (2007) From the identification of gene organization of alpha conotoxins to the cloning of novel toxins. *Toxicon* **49**, 1135-1149
34. Peng, C., Chen, W., Sanders, T., Chew, G., Liu, J., Hawrot, E., and Chi, C. (2010) Chemical synthesis and characterization of two alpha4/7-conotoxins. *Acta Biochim Biophys Sin (Shanghai)* **42**, 745-753
35. Wuthrich, K. (1986) *NMR of Proteins and Nucleic Acids*. John Wiley & Sons Inc., New York.
36. Park, K. H., Suk, J. E., Jacobsen, R., Gray, W. R., McIntosh, J. M., and Han, K. H. (2001) Solution conformation of alpha-conotoxin EI, a neuromuscular toxin specific for the alpha 1/delta subunit interface of torpedo nicotinic acetylcholine receptor. *J Biol Chem* **276**, 49028-49033
37. Chi, S. W., Kim, D. H., Olivera, B. M., McIntosh, J. M., and Han, K. H. (2004) Solution conformation of alpha-conotoxin GIC, a novel potent antagonist of alpha3beta2 nicotinic acetylcholine receptors. *Biochem J* **380**, 347-352
38. Dutertre, S., and Lewis, R. J. (2006) Toxin insights into nicotinic acetylcholine receptors. *Biochem Pharmacol* **72**, 661-670
39. Le Novere, N., Corringer, P. J., and Changeux, J. P. (2002) The diversity of subunit composition in nAChRs: evolutionary origins, physiologic and pharmacologic consequences. *J Neurobiol* **53**, 447-456
40. Tsetlin, V. I., and Hucho, F. (2004) Snake and snail toxins acting on nicotinic acetylcholine receptors: fundamental aspects and medical applications. *FEBS Lett* **557**, 9-13
41. Dutertre, S., and Lewis, R. J. (2004) Computational approaches to understand alpha-conotoxin interactions at neuronal nicotinic receptors. *Eur J Biochem* **271**, 2327-2334
42. Brejc, K., van Dijk, W. J., Klaassen, R. V., Schuurmans, M., van Der Oost, J., Smit, A. B., and Sixma, T. K. (2001) Crystal structure of an ACh-binding protein reveals the ligand-binding domain of nicotinic receptors. *Nature* **411**, 269-276
43. Armishaw, C., Jensen, A. A., Balle, T., Clark, R. J., Harpsoe, K., Skonberg, C., Liljefors, T., and Stromgaard, K. (2009) Rational design of alpha-conotoxin analogues targeting alpha7 nicotinic acetylcholine receptors: improved antagonistic activity by incorporation of proline derivatives. *J Biol Chem* **284**, 9498-9512
44. Dutertre, S., Ulens, C., Buttner, R., Fish, A., van Elk, R., Kendel, Y., Hopping, G., Alewood, P. F., Schroeder, C., Nicke, A., Smit, A. B., Sixma, T. K., and Lewis, R. J. (2007) AChBP-targeted alpha-conotoxin correlates distinct binding orientations with nAChR subtype selectivity. *EMBO J* **26**, 3858-3867
45. Marx, U. C., Daly, N. L., and Craik, D. J. (2006) NMR of conotoxins: structural features and an analysis of chemical shifts of post-translationally modified amino acids. *Magn Reson Chem* **44 Spec No**, S41-50
46. Hu, S. H., Gehrman, J., Guddat, L. W., Alewood, P. F., Craik, D. J., and Martin, J. L. (1996) The 1.1 A crystal structure of the neuronal acetylcholine receptor antagonist, alpha-conotoxin PnIA from *Conus pennaceus*. *Structure* **4**, 417-423
47. Hu, S. H., Gehrman, J., Alewood, P. F., Craik, D. J., and Martin, J. L. (1997) Crystal structure at 1.1 A resolution of alpha-conotoxin PnIB: comparison with alpha-conotoxins PnIA and GI. *Biochemistry* **36**, 11323-11330
48. Loughnan, M. L., Nicke, A., Jones, A., Adams, D. J., Alewood, P. F., and Lewis, R. J. (2004) Chemical and functional identification and characterization of novel sulfated alpha-conotoxins from the cone snail *Conus anemone*. *J Med Chem* **47**, 1234-1241
49. Talley, T. T., Olivera, B. M., Han, K. H., Christensen, S. B., Dowell, C., Tsigelny, I., Ho, K. Y., Taylor, P., and McIntosh, J. M. (2006) Alpha-conotoxin OmIA is a potent ligand for the

- acetylcholine-binding protein as well as  $\alpha 3\beta 2$  and  $\alpha 7$  nicotinic acetylcholine receptors. *J Biol Chem* **281**, 24678-24686
50. Nicke, A., Loughnan, M. L., Millard, E. L., Alewood, P. F., Adams, D. J., Daly, N. L., Craik, D. J., and Lewis, R. J. (2003) Isolation, structure, and activity of GID, a novel  $\alpha 4/7$ -conotoxin with an extended N-terminal sequence. *J Biol Chem* **278**, 3137-3144
  51. Franco, A., Kompella, S. N., Akondi, K. B., Melaun, C., Daly, N. L., Luetje, C. W., Alewood, P. F., Craik, D. J., Adams, D. J., and Mari, F. (2012) RegIIA: an  $\alpha 4/7$ -conotoxin from the venom of *Conus regius* that potently blocks  $\alpha 3\beta 4$  nAChRs. *Biochem Pharmacol* **83**, 419-426
  52. Inserra, M. C., Kompella, S. N., Vetter, I., Brust, A., Daly, N. L., Cuny, H., Craik, D. J., Alewood, P. F., Adams, D. J., and Lewis, R. J. (2013) Isolation and characterization of  $\alpha$ -conotoxin LsIA with potent activity at nicotinic acetylcholine receptors. *Biochem Pharmacol* **86**, 791-799
  53. Whiteaker, P., Christensen, S., Yoshikami, D., Dowell, C., Watkins, M., Gulyas, J., Rivier, J., Olivera, B. M., and McIntosh, J. M. (2007) Discovery, synthesis, and structure activity of a highly selective  $\alpha 7$  nicotinic acetylcholine receptor antagonist. *Biochemistry* **46**, 6628-6638
  54. Dowell, C., Olivera, B. M., Garrett, J. E., Staheli, S. T., Watkins, M., Kuryatov, A., Yoshikami, D., Lindstrom, J. M., and McIntosh, J. M. (2003)  $\alpha$ -conotoxin PIA is selective for  $\alpha 6$  subunit-containing nicotinic acetylcholine receptors. *J Neurosci* **23**, 8445-8452
  55. Martinez, J. S., Olivera, B. M., Gray, W. R., Craig, A. G., Groebe, D. R., Abramson, S. N., and McIntosh, J. M. (1995)  $\alpha$ -Conotoxin EI, a new nicotinic acetylcholine receptor antagonist with novel selectivity. *Biochemistry* **34**, 14519-14526
  56. Lewis, R. J., Dutertre, S., Vetter, I., and Christie, M. J. (2012) *Conus* venom peptide pharmacology. *Pharmacol Rev* **64**, 259-298
  57. Lluisma, A. O., Lopez-Vera, E., Bulaj, G., Watkins, M., and Olivera, B. M. (2008) Characterization of a novel  $\psi$ -conotoxin from *Conus parius* Reeve. *Toxicon* **51**, 174-180
  58. Teichert, R. W., Rivier, J., Torres, J., Dykert, J., Miller, C., and Olivera, B. M. (2005) A uniquely selective inhibitor of the mammalian fetal neuromuscular nicotinic acetylcholine receptor. *J Neurosci* **25**, 732-736
  59. Groebe, D. R., Dumm, J. M., Levitan, E. S., and Abramson, S. N. (1995)  $\alpha$ -Conotoxins selectively inhibit one of the two acetylcholine binding sites of nicotinic receptors. *Mol Pharmacol* **48**, 105-111
  60. Sine, S. M., and Claudio, T. (1991)  $\gamma$ - and  $\delta$ -subunits regulate the affinity and the cooperativity of ligand binding to the acetylcholine receptor. *J Biol Chem* **266**, 19369-19377
  61. Changeux, J. P. (1990) The TiPS lecture. The nicotinic acetylcholine receptor: an allosteric protein prototype of ligand-gated ion channels. *Trends Pharmacol Sci* **11**, 485-492
  62. Sine, S. M. (1993) Molecular dissection of subunit interfaces in the acetylcholine receptor: identification of residues that determine curare selectivity. *Proc Natl Acad Sci U S A* **90**, 9436-9440
  63. Prince, R. J., and Sine, S. M. (1996) Molecular dissection of subunit interfaces in the acetylcholine receptor. Identification of residues that determine agonist selectivity. *J Biol Chem* **271**, 25770-25777

*Acknowledgements*—We would like to thank to L. Sivilotti for sharing the  $\alpha 3$  and  $\beta 4$  cDNA. We are grateful to V. Witzemann for sharing the  $\alpha 1$ ,  $\beta 1$ ,  $\gamma$ ,  $\delta$ ,  $\epsilon 1$  clones and to J. Lindstrom for kindly providing the  $\alpha 4$  and  $\beta 2$  clones. We thank F. Clementi for sharing  $\alpha 5$  and for  $\alpha 7$ .

## FOOTNOTES

JT was supported by the following grants: G.0433.12, G.A071.10N and G.0257.08 (F.W.O. Vlaanderen), EU –FP7 – MAREX, IUAP 7/10 (Inter-University Attraction Poles Program, Belgian

State, Belgian Science Policy) and OT/12/081 (KU Leuven). Dr. M. Maiti is a postdoctoral research fellow of F.W.O. Vlaanderen, Belgium.

To whom correspondence should be addressed: Jan Tytgat, Department of Pharmacy, Toxicology and Pharmacology, KU Leuven, Herestraat 49, 3000 Leuven, Belgium, Tel: +32 16 32 34 04; Fax: +32 16 32 34 05; Email: [jan.tytgat@pharm.kuleuven.be](mailto:jan.tytgat@pharm.kuleuven.be).

<sup>1</sup>Toxicology and Pharmacology, University of Leuven (KU Leuven), Campus Gasthuisberg, O&N2, Herestraat 49, PO Box 922, 3000 Leuven, Belgium

<sup>2</sup>Medicinal Chemistry, University of Leuven (KU Leuven), Rega Institute for Medical Research, Minderbroedersstraat 10, 3000 Leuven, Belgium

<sup>3</sup>CSIR-National Institute of Oceanography, Dona Paula, Goa, India

<sup>4</sup>Center of Advanced Study in Marine Biology, Annamalai University, Parangipettai, Tamil Nadu, India

<sup>5</sup>Laboratory for Protein Phosphorylation and Proteomics, O&N1 Herestraat 49, Box 901, 3000 Leuven, Belgium

<sup>6</sup>The abbreviations used were: ACh, Acetylcholine; AChBP, Acetylcholine binding protein; ADHD, Attention Deficit Hyperactivity Disorder; IC<sub>50</sub>, Half-maximal inhibitory concentration; MALDI-TOF, Matrix-assisted laser desorption/ionization - time of flight; nAChR, Nicotinic Acetylcholine Receptor; NMR, Nuclear magnetic resonance; NOE, Nuclear Overhauser Effect; NOESY, Nuclear Overhauser Effect Spectroscopy; RMSD, Root mean square deviation; RP-HPLC, Reverse phase-high performance liquid chromatography; S.D., Standard deviation; TFA, trifluoroacetic acid

## TABLE LEGENDS

**TABLE 1.** NMR structure determination statistics of  $\alpha$ -conotoxin Lo1a for an ensemble of 15 structures. Values where applicable are the means  $\pm$  S.D.

**TABLE 2.** Alignment of 40  $\alpha$ 4/7 conotoxins with Lo1a, sorted from bottom to top by percentage of similarity with Lo1a. Percentage of similarity is indicated in the left column.

Table 1

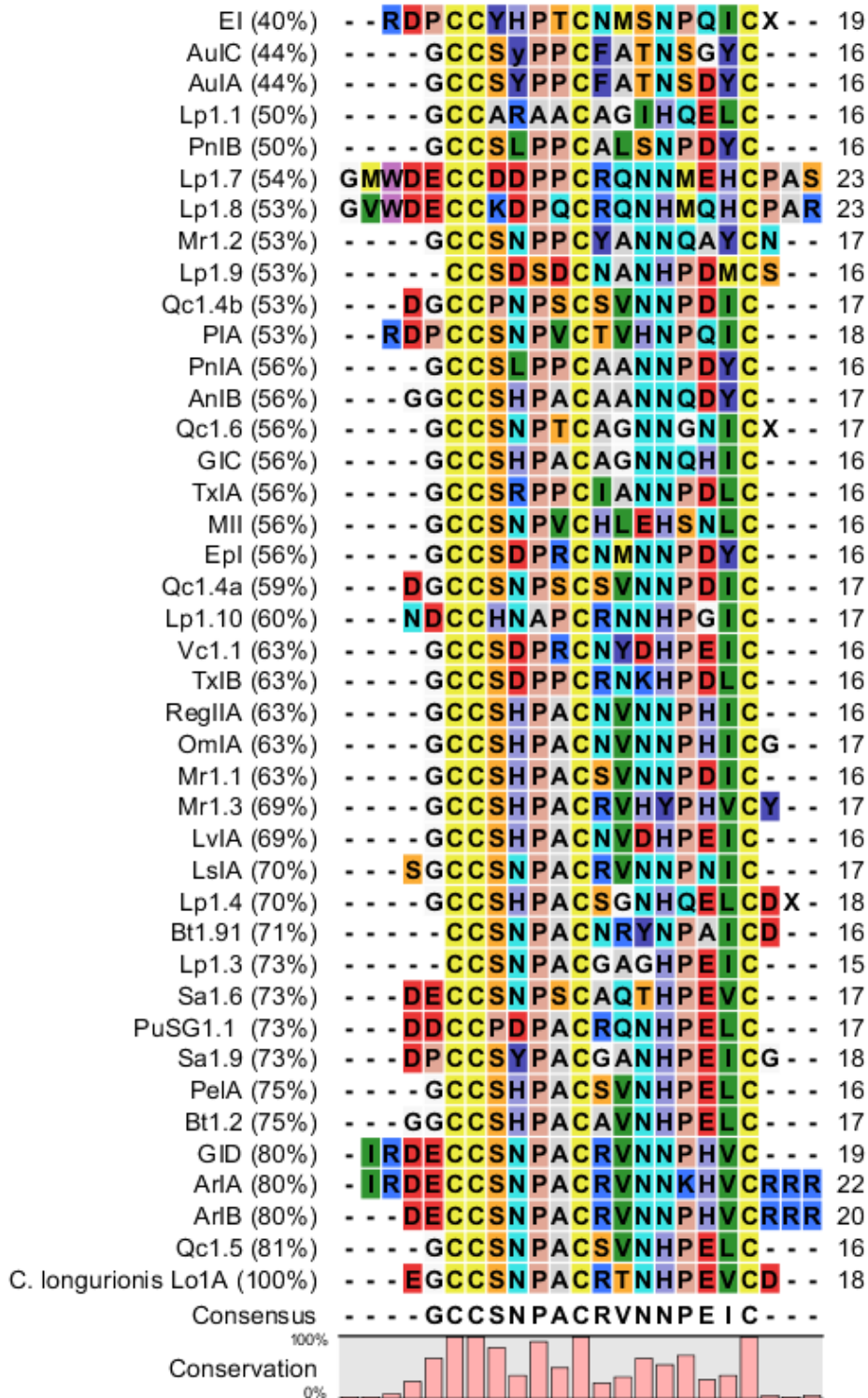


Table 2

<b>Total NOE distance restraints</b>	190
Intra residue	65
Sequential ( $ i-j =1$ )	66
Medium range ( $2 \leq  i-j  \leq 4$ )	46
Long range ( $ i-j  \geq 5$ )	13
<b>Dihedral angle restraints</b>	10 ( $\varphi=8, \omega_{X-Pro}=2$ )
<b>RMSD from the average structure (Å)</b>	
<b>Residue 3-17</b>	
Backbone atoms (N, C <sup>α</sup> , C <sup>γ</sup> )	0.43 ± 0.09
All heavy atoms	0.83 ± 0.13
<b>RMS deviation from the idealized covalent geometry</b>	
Bond (Å)	0.000008 ± 0.000000
Angle (°)	3.809 ± 0.074
Improper (°)	3.245 ± 0.412
<b>Ramachandran analysis (%)</b>	
Residues in favored regions	63
Residues in additional allowed regions	30.3
Residues in generously allowed regions	6.7
Residues in disallowed regions	0

## FIGURE LEGENDS

**FIGURE 1.** Electrophysiological profile of Lo1a. During recordings, oocytes were continuously perfused with ND96-A (ND96 with 1  $\mu\text{M}$  atropine; except for oocytes expressing  $\alpha_7$  nAChR) at a rate of 2 mL/min, with 10  $\mu\text{M}$  Lo1a applied during 30s before ACh was added. ACh (200  $\mu\text{M}$  for  $\alpha_7$ , 70  $\mu\text{M}$  for  $\alpha_3\beta_4$ , 50  $\mu\text{M}$  for  $\alpha_4\beta_2$  and  $\alpha_4\beta_4$ , 10  $\mu\text{M}$  for  $\alpha_1\beta_1\gamma\delta$  and  $\alpha_1\beta_1\gamma\epsilon$ ) was applied for 2s at 2 mL/min, with 30s washout periods between different ACh applications and 200s after toxin application.

**FIGURE 2.** Concentration-response curve on  $\alpha_7$  nAChR. Different concentration of Lo1a ( $\square$ ), Lo1a- $\Delta\text{D}$  ( $\circ$ ) and Lo1a-RRR ( $\Delta$ ) were tested on  $\alpha_7$ . The corresponding  $\text{IC}_{50}$  values are:  $3.24 \pm 0.70 \mu\text{M}$ ,  $0.80 \pm 0.01 \mu\text{M}$  and  $1.06 \pm 0.00 \mu\text{M}$  respectively. Currents were obtained as described under "Materials and Methods". The percentage of block was plotted against the logarithm of the tested concentrations. The results were fit with the Hill equation.

**FIGURE 3.** Electrophysiological profile of Lo1a- $\Delta\text{D}$ . During recordings, oocytes were continuously perfused with ND96-A (ND96 with 1  $\mu\text{M}$  atropine; except for oocytes expressing  $\alpha_7$  nAChR) at a rate of 2 mL/min, with 10  $\mu\text{M}$  Lo1a- $\Delta\text{D}$  applied during 30s before ACh was added. ACh (200  $\mu\text{M}$  for  $\alpha_7$ , 70  $\mu\text{M}$  for  $\alpha_3\beta_4$ , 50  $\mu\text{M}$  for  $\alpha_4\beta_2$  and  $\alpha_4\beta_4$ , 10  $\mu\text{M}$  for  $\alpha_1\beta_1\gamma\delta$  and  $\alpha_1\beta_1\gamma\epsilon$ ) was applied for 2s at 2 mL/min, with 30s washout periods between different ACh applications and 200s after toxin application.

**FIGURE 4.** Electrophysiological profile of Lo1a-RRR. During recordings, oocytes were continuously perfused with ND96-A (ND96 with 1  $\mu\text{M}$  atropine; except for oocytes expressing  $\alpha_7$  nAChR) at a rate of 2 mL/min, with 10  $\mu\text{M}$  Lo1a-RRR applied during 30s before ACh was added. ACh (200  $\mu\text{M}$  for  $\alpha_7$ , 70  $\mu\text{M}$  for  $\alpha_3\beta_4$ , 50  $\mu\text{M}$  for  $\alpha_4\beta_2$  and  $\alpha_4\beta_4$ , 10  $\mu\text{M}$  for  $\alpha_1\beta_1\gamma\delta$  and  $\alpha_1\beta_1\gamma\epsilon$ ) was applied for 2s at 2 mL/min, with 30s washout periods between different ACh applications and 200s after toxin application.

**FIGURE 5.** Concentration-response curve on  $\alpha_1\beta_1\gamma\epsilon$  nAChR. Different concentration of Lo1a ( $\square$ ), Lo1a- $\Delta\text{D}$  ( $\circ$ ) and Lo1a-RRR ( $\Delta$ ) were tested on  $\alpha_1\beta_1\gamma\epsilon$ . The corresponding  $\text{IC}_{50}$  values for Lo1a- $\Delta\text{D}$  and Lo1a-RRR are:  $4.40 \pm 0.18 \mu\text{M}$  and  $1.47 \pm 0.39 \mu\text{M}$  respectively. Currents were obtained as described under "Materials and Methods". The percentage of block was plotted against the logarithm of the tested concentrations. The results were fit with the Hill equation.

**FIGURE 6.** Overview of subtype selectivity. The three peptides, Lo1a, Lo1a- $\Delta\text{D}$  and Lo1a-RRR were tested on 6 different nAChRs:  $\alpha_1\beta_1\gamma\epsilon$ ,  $\alpha_1\beta_1\gamma\delta$ ,  $\alpha_7$ ,  $\alpha_3\beta_2$ ,  $\alpha_3\beta_4$  and  $\alpha_4\beta_4$  at a concentration of 10 $\mu\text{M}$ . Data are represented as the means  $\pm$  S.E. (indicated by error bars); each experiment was performed at least three times ( $n \geq 3$ ).

**FIGURE 7.** Sequence and disulfide connectivity of  $\alpha$ -conotoxin Lo1a along with a summary of short and medium range NOEs,  $^3J_{\text{HNH}\alpha}$  ( $^3J_{\alpha\text{N}}$ ) couplings, and chemical shift index (CSI) for the H $\alpha$  protons. The thickness of the bar represents relative strength of NOEs (strong, medium and weak).  $\bullet$   $^3J_{\text{HNH}\alpha} < 6$  Hz,  $\circ$   $^3J_{\text{HNH}\alpha} = 6-8$  Hz,  $\odot$   $^3J_{\text{HNH}\alpha} > 8$  Hz. The filled squares above and below the horizontal line represent CSI values of +1 and -1 respectively. Note the presence of  $\alpha$ -helix from Pro<sup>7</sup>-Asn<sup>12</sup> which is common to all  $\alpha 4/7$  subfamily conotoxins.

**FIGURE 8.** NMR solution structure of  $\alpha$ -conotoxin Lo1a. **(A)** Stereoviews of a family of 15 final structures of  $\alpha$ -conotoxin Lo1a with superimposed backbone heavy atoms (N, CA, C $^{\prime}$ ). Disulfide bonds are shown in yellow as pseudo bonds. **(B)** Front and back ribbon views of the closest-to-average structure of  $\alpha$ -conotoxin Lo1a. Side chains heavy atoms are displayed along with residue label. The two views are related by a 180 $^{\circ}$  rotation around the vertical axis.

**FIGURE 9.** Schematic diagram of the muscle subtype AChR demonstrating the circular arrangement of the subunits and the (+) and (-) surfaces of the subunit interfaces (Adapted from Sine et al. 1995 – *Neuron* (17)). The blue cubes indicate both interfaces where antagonist and agonists can bind.

Figure 1

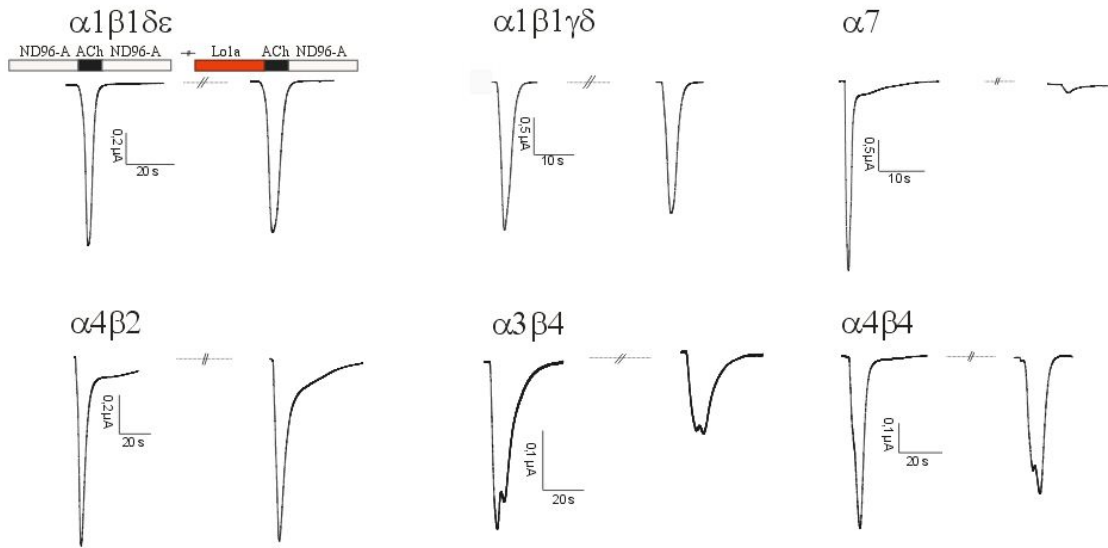




Figure 2

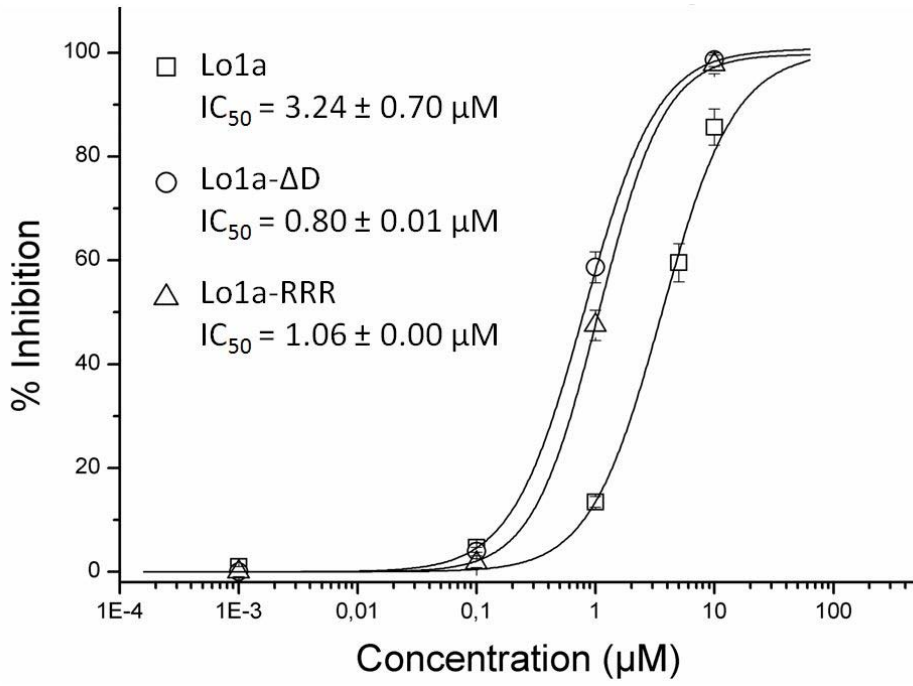


Figure 3

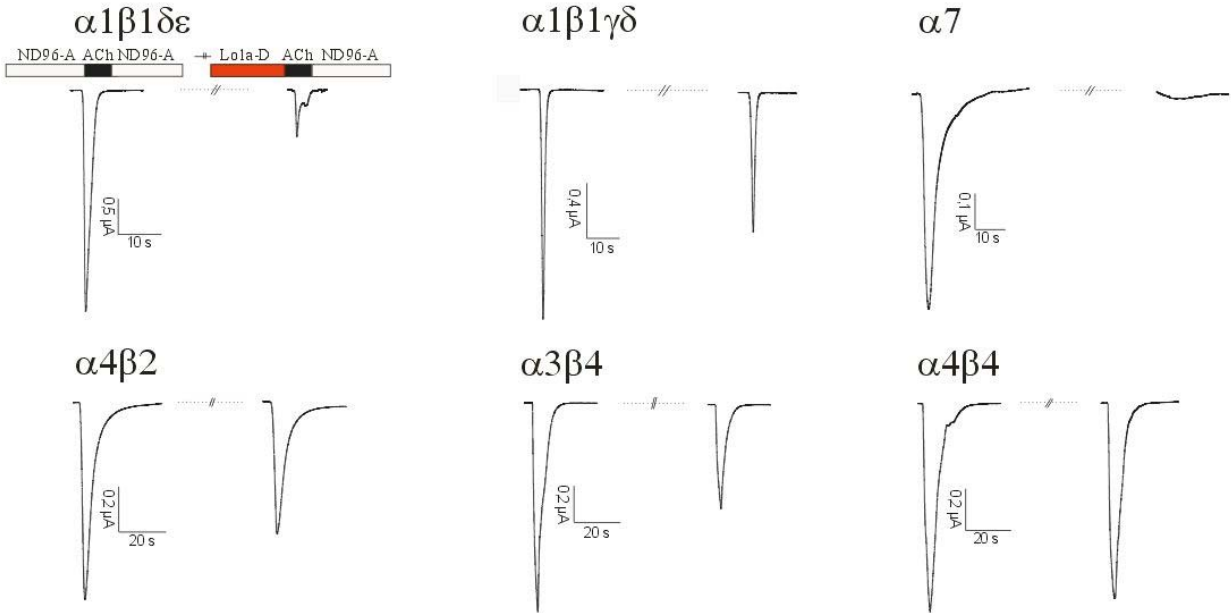
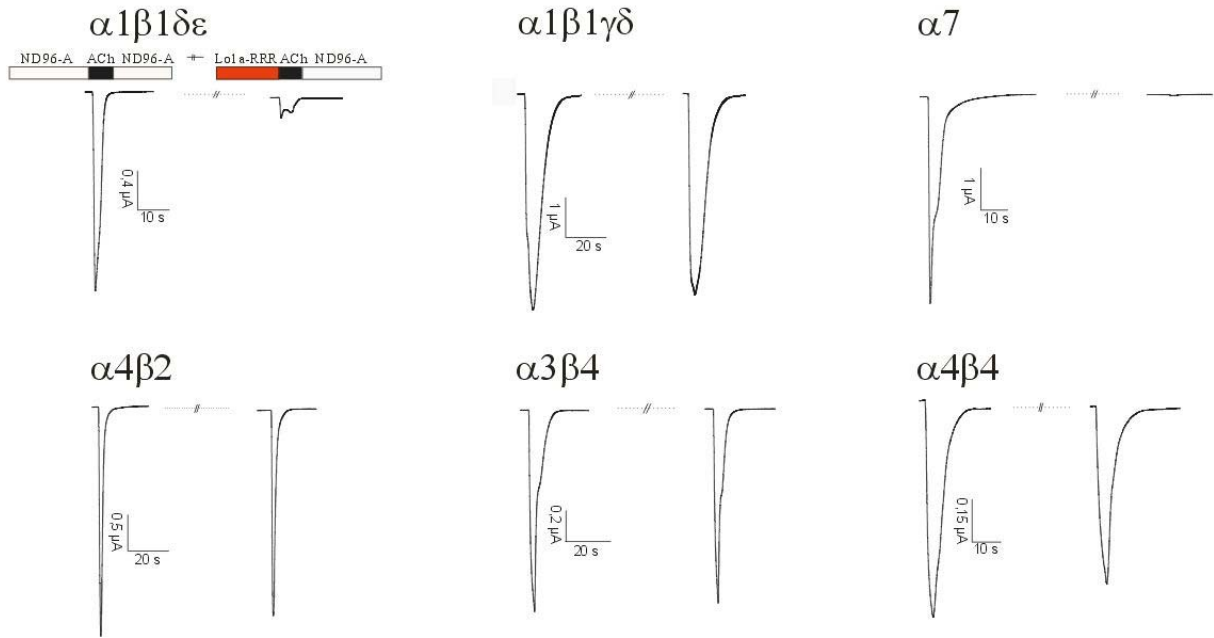


Figure 4



Figuur 5

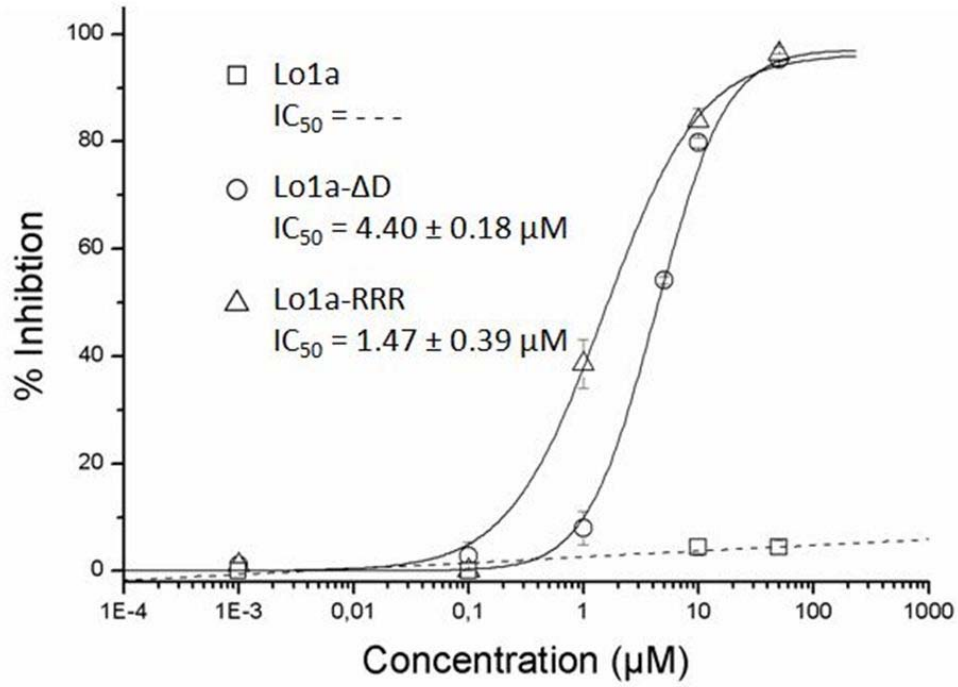


Figure 6

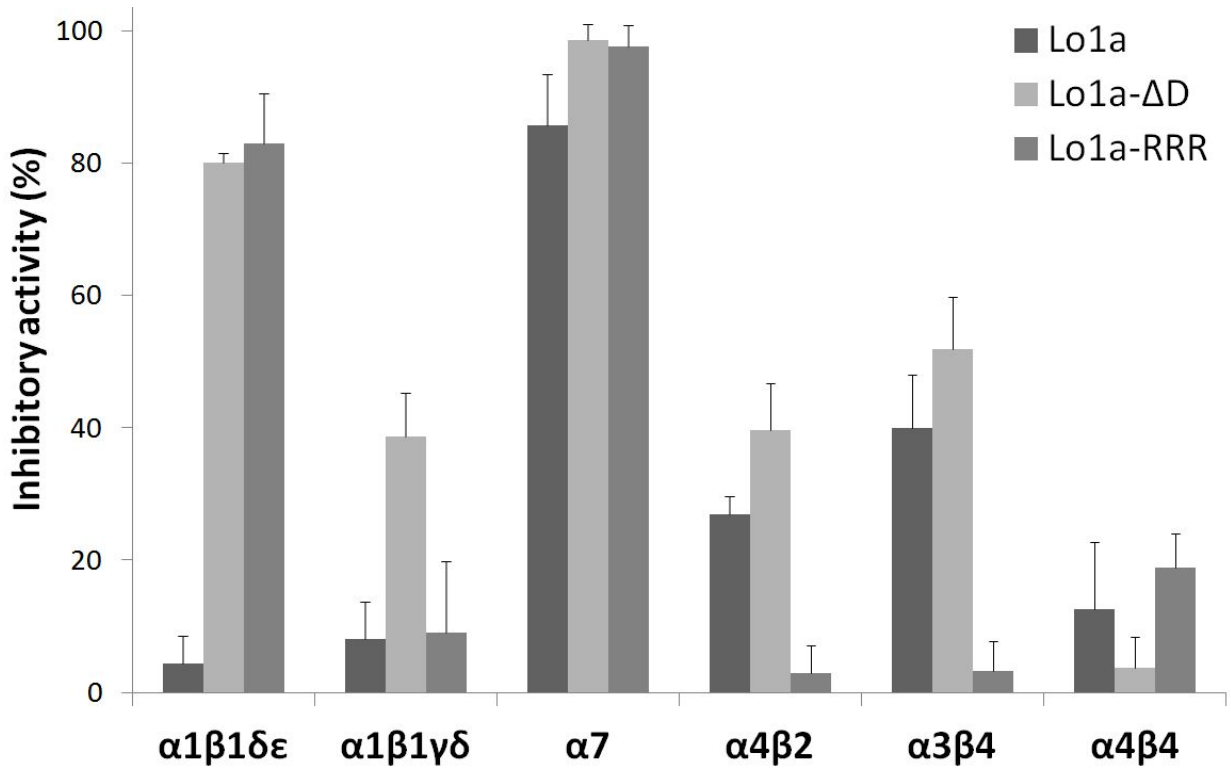


Figure 7

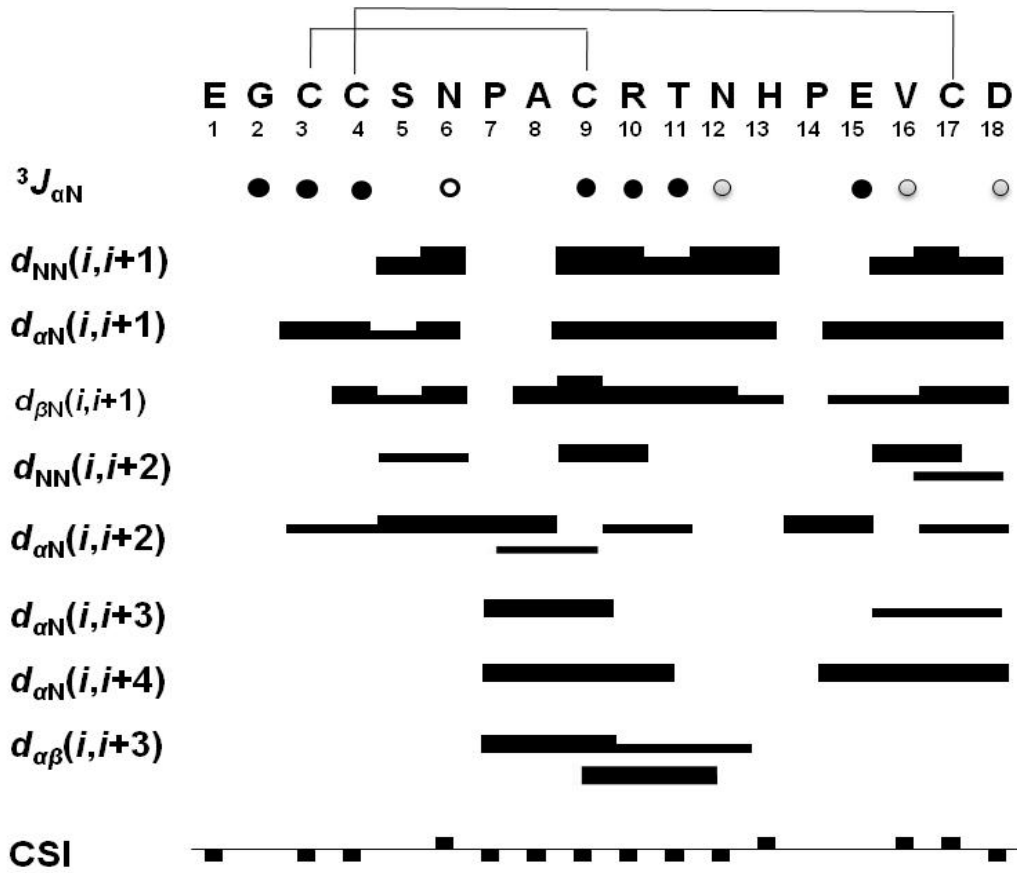




Figure 9

